Derated Mode of Power Generation in PV System Using Modified Perturb and Observe MPPT Algorithm

Vinit Kumar and Mukesh Singh

***Abstract*—In a grid-integrated photovoltaic system (GIPVS), issues such as surplus active power and inadequate performance of maximum power point tracking (MPPT) exist. A surplus active power causes the overvoltage problem at the point of common coupling in low or medium voltage level grid during the peak hours of power generation. Additionally, the inadequate performance of the MPPT technique results in the power loss due to high settling time during the sudden change in irradiance. Therefore, to solve the surplus power problem, the curtailment of active power is suggested with improved MPPT algorithm in variable irradiance conditions. In this paper, a derated power generation mode (DPGM) control strategy is presented for the curtailment of active power. Additionally, a drift free (named as modified) Perturb & Observe (P&O) is also proposed to improve the performance of the MPPT algorithm. Consequently, the DPGM control scheme with the intermediate boost converter shaves the surplus active power during the peak hours of power generation. Furthermore, the modified MPPT algorithm deals with the fluctuation of irradiance during non-peak hours. Thus, the proposed control scheme delivers in a more efficient system during the peak hours of power generation. In addition, it reduces the power loss and settling time during the change in irradiance for non-peak hours. In the support of the proposed control scheme, a 30 kW system has been simulated in the MATLAB/Simulink using Simpower tools under different environmental conditions.**

***Index Terms*—Derated power generation mode, grid integrated photovoltaic system, intermediate boost converter, modified perturb and observe, voltage source inverter.**

NOMENCLATURE

A. Abbreviations

DPGM	Derated power generation mode
GIPVS	Grid-integrated photovoltaic system
MPP	Maximum power point
MPPT	Maximum power point tracking
P-V	Power-voltage
P&O	Perturb and observe
PCC	Point of common coupling
PV	Photovoltaic
PWM	Pulse width modulation
RES	Renewable energy source
VSI	Voltage source inverter

B. Variables

ΔD	Step size of duty ratio
ΔP_{PV}	Change in PV power
ΔT	Difference of the temperature at standard test condition (STC) and actual
ΔV_{PV}	Change in PV voltage
ω	Angular frequency of the grid voltage
D	Duty ratio for boost converter
G	Operating solar irradiance
G_n	Reference solar irradiance
I_d^*, I_q^*	d-axis and q-axis reference current of the inverter
I_d, I_q	d-axis and q-axis current of the inverter
I_o	Reverse saturation current of diode
I_a, I_b, I_c	Grid side currents of the grid intigrated PV system
I_{DC}	Output current of boost converter
I_{MPP}	Current at maximum power point
I_{PV}	Current of PV array
I_{scn}	Short circuit current of PV array at standard test condition (STC)
I_{sc}	Short circuit current of PV array
k_i	Temperature co-efficient
L	Interfacing inductor at output of the inverter
m_d, m_q	d-axis and q-axis modulation indexes for the inverter
N_p	Number of PV modules in parallel
N_s	Number of PV modules in series

Manuscript received: April 20, 2019; accepted: May 15, 2020. Date of Cross-Check: May 15, 2020. Date of online publication: XX XX, XXXX.

This work was supported by the Department of Science and Technology (DST), India (No. DST/CERI/MI/SG/2017/080).

V. Kumar (corresponding author) and M. Singh are with Thapar Institute of Engineering and Technology, Patiala, Punjab, India (e-mail: vinitk72@gmail.com; mukesh.singh@thapar.edu).

DOI: 10.35833/MPCE.2019.000258

$P(t_9 - t_{16})$	Power generated from PV source in particular hours of the day
P_{DC}	Output power of boost converter
P_{limit}	Power transfer limit
P_{PV}	Power of PV array
R	Resistance of each phase
R_{in}	Input impedance of boost converter
R_{out}	Output impedance of boost converter
$S_1 - S_6$	Gate signals for the inverter
$t_9 - t_{16}$	Particular hours of the day
$t_{s,V_{MPP}}$	Settling time to meet V_{MPP}
$t_{s,V_{DC-link}^{ref}}$	Settling time to meet $V_{DC-link}^{ref}$
V_d^*, V_q^*	*d*-axis and *q*-axis reference voltage of the inverter
$V_{DC-link}^{ref}$	Reference DC-link voltage for the inverter
V_d, V_q	*d*-axis and *q*-axis voltage of the inverter
V_t	Thermal voltage of diode
$V_{DC-link}$	Measured DC-link voltage of the inverter
V_{DC}	Output voltage of boost converter
V_{MPP}	Voltage at maximum power point
V_{PV}	Voltage of PV array
V_{sa}, V_{sb}, V_{sc}	Grid side voltages of the grid intigrated PV system
V_{sd}, V_{sq}	*d*-axis and *q*-axis voltage of the grid
V_{ta}, V_{tb}, V_{tc}	Terminal voltage of the inverter

I. Introduction

In today's scenario of power generation, the acceptance of renewable energy sources (RESs) are increasing due to the shortcoming of fossil fuels. Therefore, the RESs are supporting the power generation. The RESs include wind energy, solar energy, hydro energy, fuel cell and tidal energy. Among these RESs, installation of photovoltaic (PV) solar system is advantageous due to low-cost maintenance. Therefore, the acceptance of the PV systems for grid support is booming in the renewable energy market. However, the PV power generation depends upon the irradiance. It affects the power generation but can be improved by forecasting of the power as discussed in [1], [2]. Additionally, the use of PV systems has exponentially increased due to advancement in power electronics research [3]. These are utilized in various forms which are classified as stand-alone PV, grid-integrated PV and hybrid PV system. Among these, the grid-integrated PV system (GIPVS) has an advantage over others due to its bulk power transfer capability. However, the GIPVS has some disadvantages such as overvoltage at the point of common coupling (PCC) during surplus power generation. Additionally, the maximum power point tracking (MPPT) algorithm takes more settling time which causes power loss during variable irradiance condition.

The aforementioned issues affect the smooth functioning of the GIPVS. The most affecting factor to the system is the high amount of power generation during peak hours, it causes overvoltage in the grid. It also affects the safety of grid-connected network's equipment such as transformers, circuit breakers, relays or contactors (for low or high voltage application respectively) and conductors. In addition, the tracking capability of MPPT algorithms get affected due to the random change in irradiance condition. Above mentioned issues affect the performance of the system and impose an extra cost when equipment gets damaged. Therefore, a suitable control approach and the MPPT algorithm is required.

Many researchers contributed in solving the problems such as overvoltage and inadequate MPPT's performance in a GIPVS. Zhou and Bialek [4] presented a generation curtailment technique to prevent the rise of voltage and reverse power flow in the lower network from high penetration of PV power. However, the authors did not recommend any control technique to minimize the switching losses and increases the utilization of the inverter. Further, Tonkoski *et al.* [5] presented a droop based curtailment approach to protect the grid from overvoltage. Although this scheme increases the power loss as compared to normal active power curtailment, it affects the revenue of the system. Similarly, Omran *et al.* [6] suppresses the power fluctuation of GIPVS using various approaches such as battery storage, dump loads and software-based power curtailment. However, the above mentioned approaches have a high installation cost except power curtailment. Likewise, Ahmed *et al.* [7] proposed a reduced power mode control algorithm to suppress the output power of the system. It works in reduced power generation mode when generated power exceeds the system rating. Though the proposed control strategy fails to reduce the power losses during curtailment.

Yang *et al.* [8] proposed a constant power generation scheme to reduce thermal loading, improved the inverter utilization and reduced the switching losses of inverter during a rapid change in irradiance. However, the authors did not present an appropriate method to decide the power limit. In addition, Sangwongwanich *et al.* [9], [10] presented a constant power generation scheme for the overshoot, power loss and active curtailment. The authors have used the power or current based scheme for fast dynamic response and MPPT for high robustness. Although the authors didn't use any other MPPT except perturb and observe (P&O) technique. Similarly, Tafti *et al.* [11] have also proposed a constant power generation scheme for the single and two-stage three-phase GIPVS. In this scheme, the authors have proposed a voltage based curtailment approach along with the flexibility of operating points. However, the main shortcoming of this scheme was that it didn't suggest any suitable approach to decide the voltage operating point during variable irradiance. Although they have only used conventional MPPT to find the operating point.

As aforementioned, the control schemes which have been applied for the derated mode of operation during peak hours of power generation, lag to do the following:

1) Most of the existing technologies are based on conventional MPPT (P&O and Incremental Conductance) techniques.

2) Implemented systems are mostly a single phase GIPVS.

3) A proper tracking strategy has not been proposed which can reduce the power loss during the search of maximum power point (MPP).

The above-mentioned limitations can be resolved through a proposed derated power generation scheme with a modified MPPT. The proposed scheme will perform in peak as well as in non-peak hours of power generation and improves the tracking capability of the MPPT algorithm. It will resolve the problem of overvoltage and the others such as drifting, oscillation near MPP and tracking speed. As a result, the power loss during the search of operating point will be reduced under variable irradiance level. Hence, a suitable MPPT algorithm is required.

Many researchers have classified various MPPT techniques on the basis of the properties such as tracking speed [7], complexity [12], MPP oscillation [13], accuracy and efficiency [14]. Jain and Agarwal [12] have compared many classical MPPT techniques based on array configuration, accuracy, cost of the system and tracking speed. However, the authors have presented the application based MPPTs which are not applicable for every system. Esram and Chapman [15] have presented the comparison of various MPPT algorithms according to the PV application. Similarly, Subudhi and Pradhan [16] have also presented a review of many MPPT algorithms. The review is based on the control strategy, circuitry and the cost of the application. This review reflects that the P&O is less complex and having fast tracking capability amongst all presented. However, P&O is less accurate and consume more power in MPP tracking during variable irradiances. Therefore, many modified P&O MPPT algorithms have been presented to overcome the MPPT problems. In this respect, Killi and Samanta [17] have proposed a modified P&O algorithm which resolves the drift problem during unpredicted irradiance change. As a result, this MPPT presents high efficiency and less power loss during tracking of the operating point. Yong and Huiqing [18] have presented an adaptive P&O algorithm with predictive current control. However, the authors have failed to consider the inductance change which influences the tracking accuracy of the algorithm. Similarly, Ahmed and Salam [13] proposed a modified P&O algorithm with dynamic perturbation step size and a boundary condition to enhance the efficiency of the algorithm. Although this directs the system towards the operating point, it fails to handle the irradiance changes. Further, Liu *et al.* [19] and Ghamrawi *et al.* [20] have proposed a dual-mode P&O algorithm with the variable step-size which contribute to resolve the problem of oscillation near MPP and MPP tracking speed. However, the employed algorithm has a slightly higher cost as compared to the traditional P&O and unable to identify the drift problem during variable irradiance condition. Hence, a modified MPPT technique has to be proposed that can resolve the above mentioned problems.

The aforementioned issue of excess power generation during peak hours affect the distribution network. Therefore, limiting of power transfer is required during peak hours generation. The power transfer is limited by introducing the tap-changing transformer, voltage regulator, increasing the conductor size, storage and curtailment approach [5, 21]. Among all methods of power limiting, the curtailment of surplus power is the most suitable method [4]. In this respect, Omran *et al.* [6] have proposed a derated mode approach for curtailment of the surplus power. Likewise, various methods of derated mode operation are addressed in the literature. They have implemented a current, voltage, power and P&O MPPT based derated mode generation. In comparison to all, the selection of P&O based derated mode generation is most suitable due to less complexity. However, system efficiency and accuracy is less. Additionally, the algorithm oscillates near the operating point (i. e., drifting from the operating point in the random direction). Therefore, a novel MPPT technique is required to keep the system in derated mode generation with higher efficiency, accuracy, less drift and minimum power loss.

The significant contributions of this paper are summarized as follows.

1) A derated mode GIPVS has been proposed to limit the power transfer and resolve the overvoltage problem at PCC during peak power generation.

2) The proposed scheme introduces a modified MPPT which limit the power transfer.

3) This MPPT algorithm results in improved tracking speed and efficiency which reduces the power loss during variable irradiance condition.

The rest of the paper is organized in the following manner. Section II presents the system framework and its working strategy. Section III elaborates the proposed control strategy of the GIPVS. Further, the simulation results are presented in Section IV to support the proposed control strategy. Finally, the conclusion is delivered in Section V.

II. System Framwork and Working Strategy

This section briefs the system structure and proposed control strategy of GIPVS. The proposed system consists of two-stages as shown in Fig. 1. The stage one includes a PV array, boost converter and MPPT control. In the proposed system, a modified MPPT algorithm has been implemented which work in derated power generation mode (DPGM) and modified MPPT mode. The DPGM gets activated when generation exceeds the pre-defined power limit (P_{limit}), otherwise it works in modified MPPT mode [8]. Further, the modified MPPT generates a pulse width modulation (PWM) signal for the boost converter to get desired DC-link voltage level. On the other hand, in the second stage, the system is consist of an IGBT based voltage source inverter (VSI) and integrated with the grid. The interfacing inductors are used between the inverter and the grid to inject the current as well as generated power with the help of inverter control. The inverter control of the proposed system consist of a dual control loop and the grid synchronization technique. The control of the system is obtained in synchronously rotating or *dq* reference frame [22]. This consist of a direct (*d*) and quadrature (*q*) ax-

is which deals with the active and reactive power control respectively. Furthermore, the controller generates the PWM signals to trigger the VSI and transfer power. Finally, the complete system is developed and simulated for a 30 kW, two-stage, three-phase, grid integrated PV system.

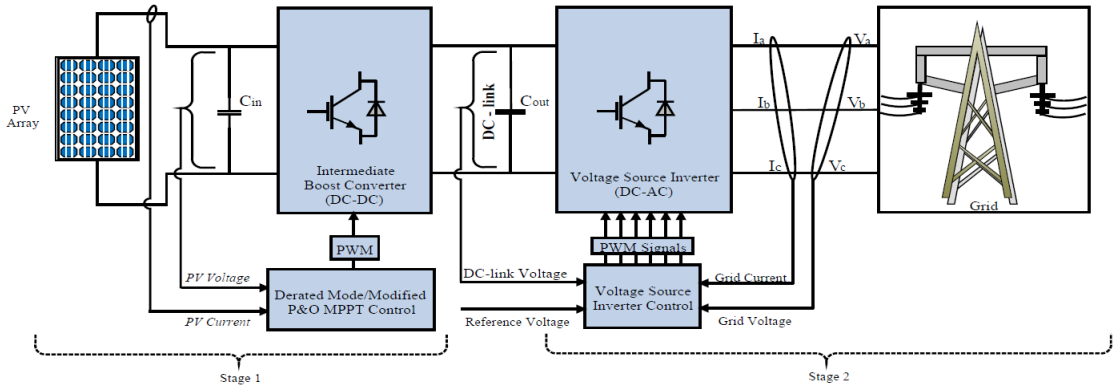

Fig. 1. Block diagram of proposed two-stage three-phase grid-integrated PV system.

III. Proposed Control Technique

In this section, the control approach of each converter used for the first and second stage of the system has been presented. In the first stage of control, the functionality of MPPT with the boost converter is illustrated in the upcoming subsections.

A. Conventional P&O MPPT Algorithm

In the MPPT technique, the extracted voltage and current from the PV source is provided to the MPPT controller as shown in Fig. 2. This controller reaches to the operating point using direct duty ratio, three-step strategy on the power-voltage (P-V) characteristic curve as shown in Fig. 3.

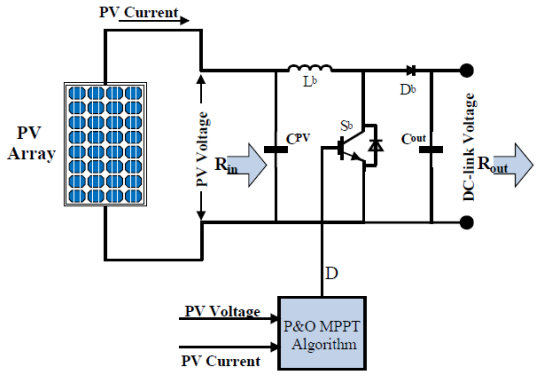

Fig. 2. Circuit diagram of DC-DC boost converter with MPPT control.

In Fig. 3, the region of the operating point depends upon the slope of the power (change in PV power i.e., ΔP_{PV}). The three-step approach is considered for the left and right region of the P-V characteristic curve. In the left region, the slope of the power is positive with respect to the voltage so it moves forward towards the operating point. On the right side, power slope is negative with respect to the voltage, therefore it moves back towards the operating point as depicted below.

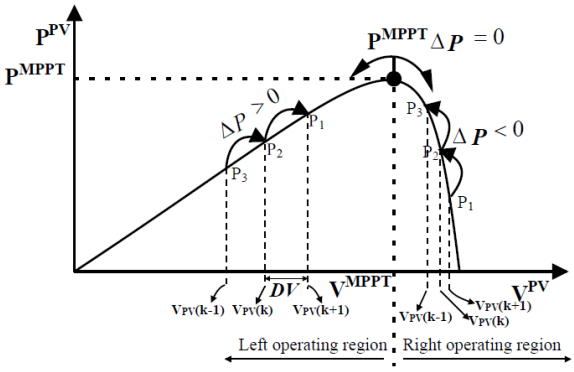

Fig. 3. Conventional P&O MPPT algorithm searching strategy.

$$\begin{cases} \dfrac{dP_{PV}}{dV_{PV}} > 0 & \text{Move forward towards MPP} \\ \dfrac{dP_{PV}}{dV_{PV}} < 0 & \text{Move back towards MPP} \\ \dfrac{dP_{PV}}{dV_{PV}} = 0 & \text{At MPP} \end{cases} \tag{1}$$

The corresponding increment and decrement in the duty ratio are due to the change in input power w. r. t. voltage. Consequently, the impact of the change in duty ratio on output voltage V_{DC} and current I_{DC} of boost converter can be illustrated as:

$$V_{DC} = \frac{1}{(1-D)} V_{PV} \tag{2}$$

$$I_{DC} = I_{PV}(1-D) \tag{3}$$

The ratio of V_{DC} and I_{DC} is the output impedance R_{out} of the boost converter which is calculated as follows.

$$R_{out} = \frac{V_{DC}}{I_{DC}} = \frac{R_{in}}{(1-D)^2} \tag{4}$$

where R_{in} and D is the input impedance and duty ratio respectively. At constant R_{in}, the value of R_{out} is inversely pro-

portional to the duty ratio. Therefore, to achieve the maximum power, voltage and current at a particular duty ratio, the value of R_{out} is depicted as

$$R_{out} = \frac{V_{MPP}}{I_{MPP}} \tag{5}$$

Moreover, the performance of P&O depends upon the increment or decrement in step size (ΔD) of duty ratio [23]. Whenever, the value of ΔD is small, the time response to achieve the MPP is more which results in power loss. On the other hand, with a large step, the time response is fast, but the drift problem occurs during the variable irradiance condition as explained in [17]. It occurs due to the lack of direction knowledge (i.e., an increase in ΔP_{PV} is due to variable irradiance or perturbation of ΔD). Therefore, the operating point gets confused about the situation that whether it should move towards the MPP or away from the MPP. Moreover, the conventional P&O only tracks the MPP during peak or non-peak hours of power generation. However, it does not participate in limiting the excess power generated during peak hours.

B. Modified P&O MPPT Algorithm

The proposed modified algorithm reduces the power loss as well as improves the time response. It also keeps the system drift-free during variable irradiance condition. In addition, the proposed MPPT limit the excess power generation during peak hours. The proposed algorithm operates in two modes such as modified MPPT mode and derated power generation mode (DPGM) as illustrated in Fig. 4. Whenever, the generated PV power is within the power transfer limit (P_{limit}), the system works in modified MPPT mode. Otherwise, the system works in DPGM as depicted below.

$$P_{DC}(t) = \begin{cases} P_{PV}(t) & \text{Modified MPPT mode for} < P_{limit} \\ P_{limit}(t) & \text{DPGM for} \geq P_{limit} \end{cases}$$

1) Modified MPPT Mode

The modified MPPT mode of the proposed algorithm follows the direct duty ratio (D), three-step strategy as mentioned in Section III-A. In this strategy, a large value of ΔD is considered for the better time response. However, the large value of ΔD creates the problem of drift during irradiance change. As discussed in [17], the current level depends upon the irradiance level, which can be explained for a single diode model PV array and related equations are depicted as follows [24], [25].

$$I_{PV} = N_p \left[I_{sc} - I_o \left\{ \exp\left(\frac{V_{PV}}{N_s V_t} \right) - 1 \right\} \right] \tag{6}$$

$$I_{sc} = N_p \left[I_{scn} + k_i (\Delta T) \right] \frac{G}{G_n} \tag{7}$$

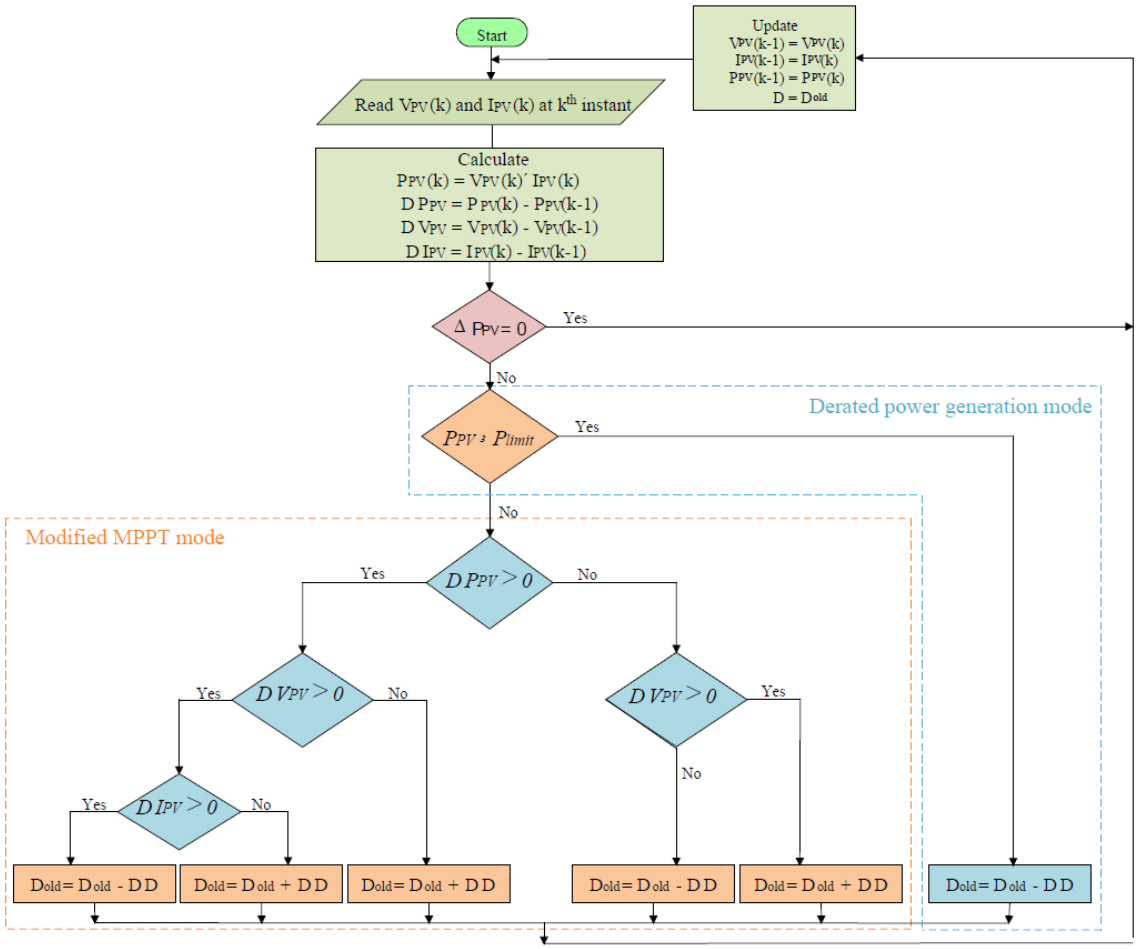

Fig.4. Flow chart of modified P&O MPPT algorithm.

where I_{sc}, I_o and V_t are the short circuit current, reverse saturation current and thermal voltage of the cell respectively. N_s and N_p present the series and parallel arrangement of modules respectively. I_{scn}, G_n, G, k_i and ΔT are the short circuit current at STC, reference irradiance, operating irradiance, temperature coefficient and difference of the temperature at actual and STC respectively. The MPP value of the PV array is delivered at particular R_{out} is depicted as:

$$I_{MPP} = N_p\left[I_{sc} - I_o\left\{\exp\left(\frac{V_{MPP}}{N_s V_t}\right) - 1\right\}\right] \tag{8}$$

By putting Taylor's expansion on (8) till first order and substituting (4) and (5), the (8) can be obtained as:

$$V_{MPP} = \frac{N_p I_{sc}}{\left[\frac{(1-D)^2}{R_{in}} + \frac{I_o N_p}{N_s V_t}\right]} \tag{9}$$

$$I_{MPP} = \frac{(1-D)^2 N_p I_{sc}}{R_{in}\left[\frac{(1-D)^2}{R_{in}} + \frac{I_o N_p}{N_s V_t}\right]} \tag{10}$$

By substituting (7) in (9) and (10), the V_{MPP} and I_{MPP} can be expressed as follows.

$$V_{MPP} = \frac{N_p^2\left[I_{scn} + k_i\Delta T\right]\frac{G}{G_n}}{\left[\frac{(1-D)^2}{R_{in}} + \frac{I_o N_p}{N_s V_t}\right]} \tag{11}$$

$$I_{MPP} = \frac{(1-D)^2 N_p^2\left[I_{scn} + k_i\Delta T\right]\frac{G}{G_n}}{R_{in}\left[\frac{(1-D)^2}{R_{in}} + \frac{I_o N_p}{N_s V_t}\right]} \tag{12}$$

where G and T are the variable parameters in (11) and (12). Therefore, the maximum value of V_{MPP} and I_{MPP} w.r.t. G is expressed as:

$$\frac{dV_{MPP}}{dG} = \frac{N_p^2\left[(I_{scn} + k_i\Delta T)\frac{1}{G_n} + \frac{G}{G_n}k_i\frac{dT}{dG}\right]}{\left[\frac{(1-D)^2}{R_{in}} + \frac{I_o N_p}{N_s V_t}\right]} \tag{13}$$

$$\frac{dI_{MPP}}{dG} = \frac{(1-D)^2 N_p^2\left[(I_{scn} + k_i\Delta T)\frac{1}{G_n} + \frac{G}{G_n}k_i\frac{dT}{dG}\right]}{R_{in}\left[\frac{(1-D)^2}{R_{in}} + \frac{I_o N_p}{N_s V_t}\right]} \tag{14}$$

Since G is increasing, I_{scn}, I_o, k_i, N_p, N_s, V_t and G_n are constant at STC and G, D and R_{in} are positive. Simultaneously, temperature also increases w. r. t. irradiance. Therefore, in (13) and (14) all the terms are positive as irradiance increases which means voltage and current are positive w.r.t. irradiance which is expressed as follows:

$$\frac{dV_{MPP}}{dG} > 0 \text{ and } \frac{dI_{MPP}}{dG} > 0$$

Similarly,

$$\frac{dV_{PV}}{dG} > 0 \text{ and } \frac{dI_{PV}}{dG} > 0$$

As mentioned above, the voltage and current increase w.r.t. irradiance. Thus, based on current, voltage and power information, the drift problem can be avoided and analysed as follows.

When irradiance is increasing, the point b shifted to point c and then shifted to d on a new P-V curve as shown in Fig. 5. In this curve, the difference between point b and d for P, V and I is positive. It can be observed that the ΔV and ΔI are positive only when irradiance is increasing. This shows that the current's information during MPP tracking is essential. Further, based on these observations, ΔV and ΔI are positive which leads to the reduction in duty ratio. Consequently, the corresponding voltage decreases as compared to the conventional P&O where the voltage used to be increased. This depicts that the operating point which is used to move away from the MPP started moving towards the MPP because of the information of current. It means that the operating point is not deviating from MPP during variable irradiance condition or in other words, not drifting away from the MPP.

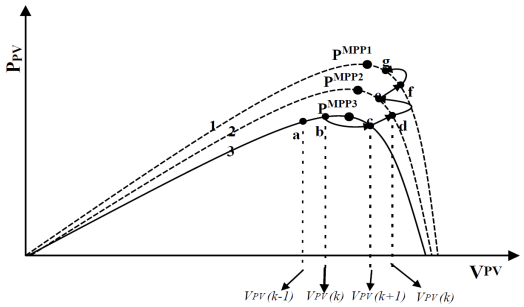

Fig. 5. Drift analysis of operating point during variable irradiance condition.

2) Derated Power Generation Mode

In derated power generation mode, the modified P&O MPPT algorithm gets activated during available surplus power. As it is known that the peak power rating of the installed PV array is always more than the average power generated during the whole day. Thus, the PV array generates surplus power during peak hours. Therefore, to remove the surplus power, a power limit is required within which the power can be transferred without affecting the distribution network equipment. In this paper, a power limit P_{limit} has been considered which is the average of power generated during 9 to 16 hours of the day and is presented as follows.

$$P_{limit}(t) = \frac{P(t_9) + P(t_{10}) + ... + P(t_{16})}{t_9 + t_{10} + ... + t_{16}} \tag{15}$$

where $P(t_9), P(t_{10}), ..., P(t_{16})$ are the peak powers generated during $t_9, t_{10}, ..., t_{16}$ respectively. When the generated power exceeds the P_{limit}, the derated mode turns on and shaves the surplus power. In Fig. 6, the power curve is within the limit at every time instant which shows the active participation of DPGM.

Based on the above discussions in Section III-A and III-B, the conventional and proposed MPPT algorithms with boost converter generates the DC power in first stage control. Further, in second stage control, the generated DC power is provided to the VSI for power conversion with inverter control which has been discussed in the next subsection.

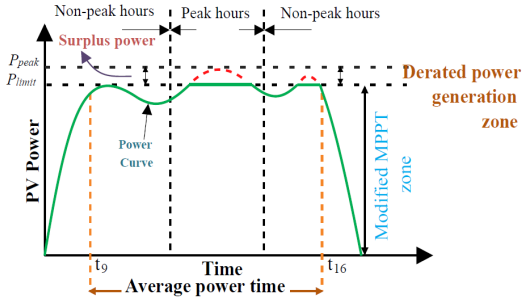

Fig.6. Day time power profile of a PV array.

C. Inverter Control for Grid Integration

The generated DC power is converted into AC power using VSI. The obtained AC power is further injected into the grid with the help of inverter control as shown in Fig. 7. In this process, the inverter control performs voltage regulation, current control and grid synchronization in synchronous (*dq*) reference frame. The voltage regulation or outer loop produces the reference current I_d^*. In this loop, the DC-link voltage is compared with a pre-defined reference voltage using a proportional-integral (PI) controller which produces I_d^* as shown in Fig. 8. On the other hand, in the inner loop, the decoupled current control scheme is used to generate the gate pulses for the VSI. In this technique, I_d^* is taken as the reference current for the active power control. Similarly, I_q^* is the reference current for reactive power control which is set as zero to transfer the power at unity power factor. Furthermore, both active and reactive power controllers generate the modulating signals as shown in Fig. 9. The respective mathematical modelling of the system as per Fig. 7 is depicted below [26].

$$\frac{dI_{abc}}{dt} = -\frac{R}{L} I_{abc} + \frac{1}{L}(V_{tabc} - V_{sabc}) \tag{16}$$

where R, L, V_{tabc}, V_{sabc} and I_{abc} are the resistance, interfacing inductance, inverter terminal voltage, grid voltage and the current respectively.The mathematical expressions of the system are of a higher degree in the natural reference frame (*abc*). Therefore, to use a simple controller (i.e., PI) and less mathematical complexity, the present reference frame (*abc*) is transformed into rotating reference frame (*dq*) using Park's transform [27] and the resultant equations are illustrated as:

$$\frac{dI_{dq}}{dt} = -\frac{R}{L} I_{dq} \pm \omega I_{qd} + \frac{1}{L}(V_{tdq} - V_{sdq}) \tag{17}$$

Or:

$$L\frac{dI_{dq}}{dt} = -RI_{dq} + V_{dq}^* \tag{18}$$

$$V_{dq}^* = V_{tdq} - V_{sdq} \pm \omega L I_{qd} \tag{19}$$

where ω is the angular frequency of the grid voltage. As mentioned in [28], the terminal voltage of inverter requires input DC-link voltage and modulation index. Hence, in *dq*-reference frame, the modulation index is presented as follows.

$$V_{tdq} = m_{dq}\frac{V_{DC}}{2} \tag{20}$$

Now, substituting (20) in (19) to get the modulating signals which is depicted as follows.

$$m_{dq} = \frac{2}{V_{DC}}(V_{dq}^* \mp \omega L I_{qd} + V_{sdq}) \tag{21}$$

These modulating signals m_d and m_q have been transformed from $dq \rightarrow abc$ to provide the gate signals $(S_1 - S_6)$ to the VSI which generates voltage and current. Since the power has to be transferred in the grid, the generated voltage and current should be in phase. Therefore, a phase-locked loop technique has been added in the system which synchronize the VSI's generated voltage and current with the grid.

Finally, in the next Section, the performance of the control approaches are evaluated and verified in the MATLAB/ Simulink environment.

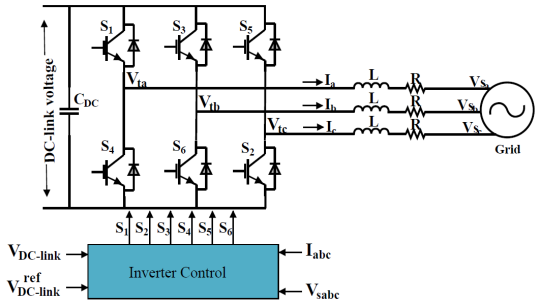

Fig. 7. Circuit diagram of VSI with grid integration.

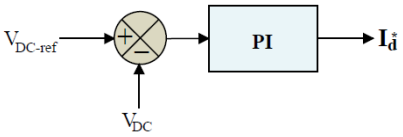

Fig. 8. Voltage regulation/outer loop of inverter control.

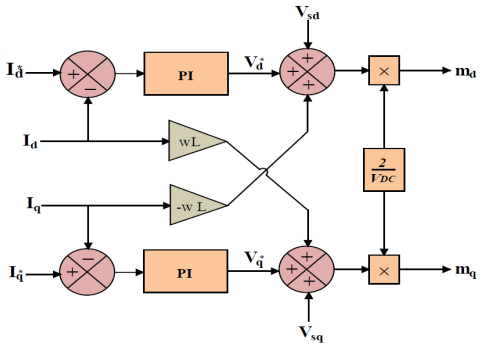

Fig. 9. Current control/inner loop of the inverter control.

IV. Simulation Results

A 30 kW, two-stage, three-phase, grid-integrated PV system using modified P&O MPPT algorithm is simulated in

MATLAB/Simulink environment with Simpower tools. The modified MPPT performs derated power generation which restricts the power generation when it reaches to or beyond the P_{limit}. Simultaneously, the conventional P&O algorithm is also examined to select a suitable ΔD for the modified P&O algorithm under variable irradiance condition. Thereafter, the performance of the conventional and modified P&O algorithm are analysed in terms of PV power, PV voltage, duty ratio, DC-link and output power as follows.

A. Conventional P&O MPPT Algorithm

For the evaluation of input voltage deviation and time response, the conventional P&O algorithm is tested for different values of ΔD. Simultaneously, to test the robustness of the system, the algorithm is evaluated under variable irradiance condition. For the sake of evaluation, a small step size $\Delta D = 3e^{-7}$ and a big step size $\Delta D = 3e^{-4}$ are considered. Now, it can be observed from Fig. 10(a) and (b) that due to the large step size, the oscillation in input voltage is significant. Furthermore, it is evident that the duty ratio achieves a steady state condition in less time under variable irradiance condition which is shown in Fig. 10. Hence, it can be concluded that the fast dynamic response can be achieved through a large step size. However, the operating point oscillates near the MPP due to large step size. To remove the oscillation near MPP, a modified P&O algorithm is adopted.

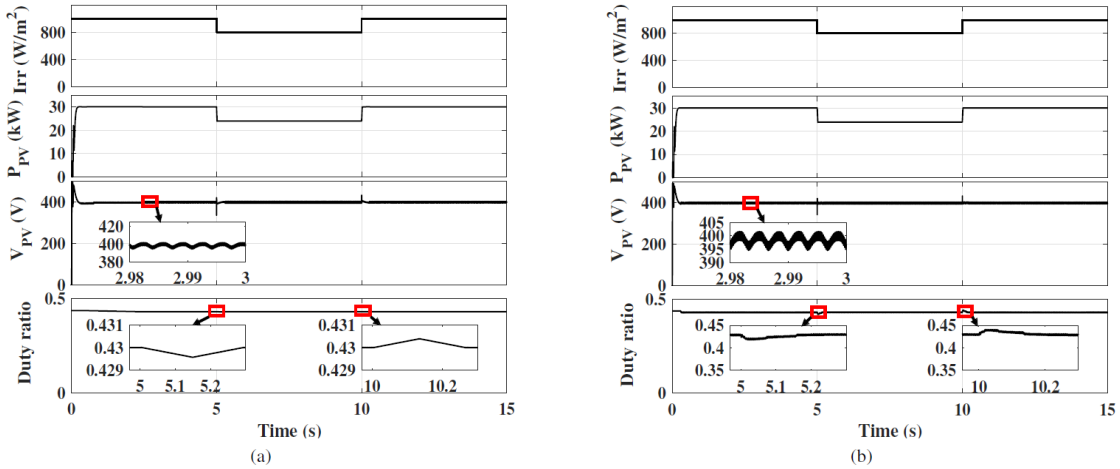

Fig. 10. Steady state performance of conventional P&O algorithm. (a) At $\Delta D = 3e^{-7}$. (b) At $\Delta D = 3e^{-4}$.

B. Modified P&O MPPT Algorithm

The performance of the modified P&O algorithm is evaluated in two modes. One is a modified MPPT mode and another is derated power generation mode.

1) Modified MPPT Mode

In this mode, the modified MPPT works like the conventional P&O until power generation does not reach to the power limit. Besides, the modified algorithm provides the right direction and less variation in voltage of the operating point towards MPP. Figure 11(a) depicts that the variation in V_{PV} which is less as compared to the conventional P&O. Simultaneously, the change in the duty ratio is positive when irradiance is increasing as discussed in modified MPPT mode of Section III. On the other hand, when irradiance is decreasing, the current decreases so the input voltage and corresponding duty ratio increases. Thus, the V_{PV} does not deviate and reaches to the operating point. In addition, the effect of irradiance change in DC-link voltage, phase voltage (V_a) and current (I_a) is shown in Fig. 11(b).

2) Derated Power Generation Mode

The system enters in derated power generation mode when the net power generation exceeds the power limit. During this mode, the modified P&O MPPT algorithm curtails the excess power. A power profile is presented in Fig. 6 which is based on the irradiance change between morning to evening time. In this paper, the system is simulated for t=15 s where one second scaled as one hour of the day to replicate the peak and non-peak hours of the power profile. Now, Fig. 12(a) depicts that the system starts generating power from t=0 and it enters into the peak-hours zone after t=5 s. In this zone, the excess power is shaved using modified MPPT and it remains in this mode till t=9 s. In this time, the system generates P_{limit} of 24 kW, which is the average power during 9 to 16 hours. During this time, the system performs in a derated power generation mode. Furthermore, the performance of V_{PV}, duty ratio, DC-link voltage, grid voltage and current are presented in Fig. 12(b).

C. Statical Analysis

Further, to analyse the performance of proposed modified P&O and conventional P&O algorithm, a statical analysis has been presented in Table I, where SD is the standard deviation. The statical analysis is presented in terms of mean and standard deviation (SD) of the settling time to meet V_{MPP} and $V_{DC-link}^{ref}$ of the system. In this respect, 30 trial runs are carried out to analyse the performance of both the algorithms at constant and variable irradiance conditions. The trial runs are performed at constant irradiance condition i.e. 600 W/m^2 for t=6s. Whereas, in variable irradiance condition at t=1.5s, it changes from 600 W/m^2 to 400 W/m^2 and back from 400 W/m^2 to 600 W/m^2 at t=3s. Table I is evident of the trial's outcome in the form of mean and SD of the settling time. The mean result of the proposed algorithm is better than the

conventional algorithm. Simultaneously, the SD result's of the proposed algorithm appear almost zero for constant as well as variable irradiance condition. The above mentioned results indicate the high robustness and search capability of the proposed modified P&O algorithm.

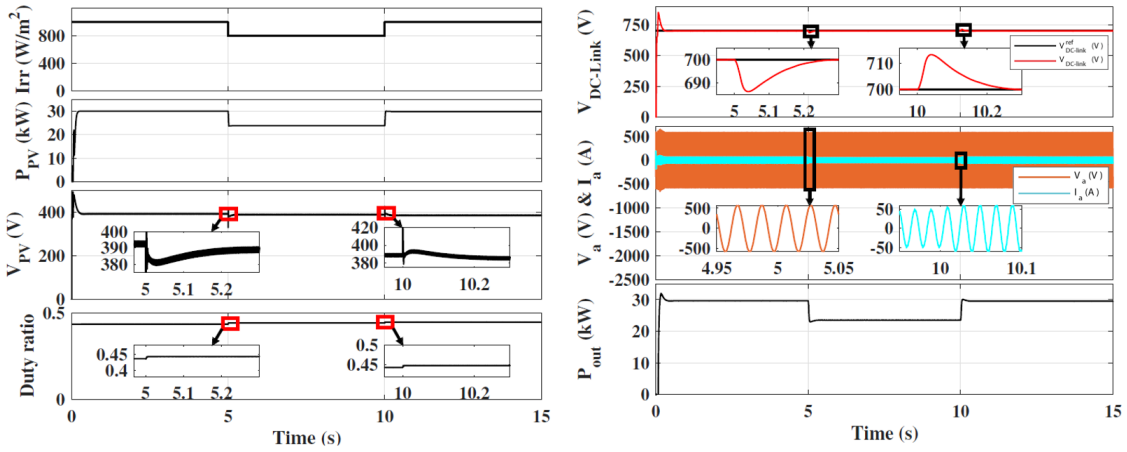

Fig. 11. Dynamic performance of modified P&O algorithm in modified MPPT mode. (a) PV source output performances. (b) DC-link and inverter output performances.

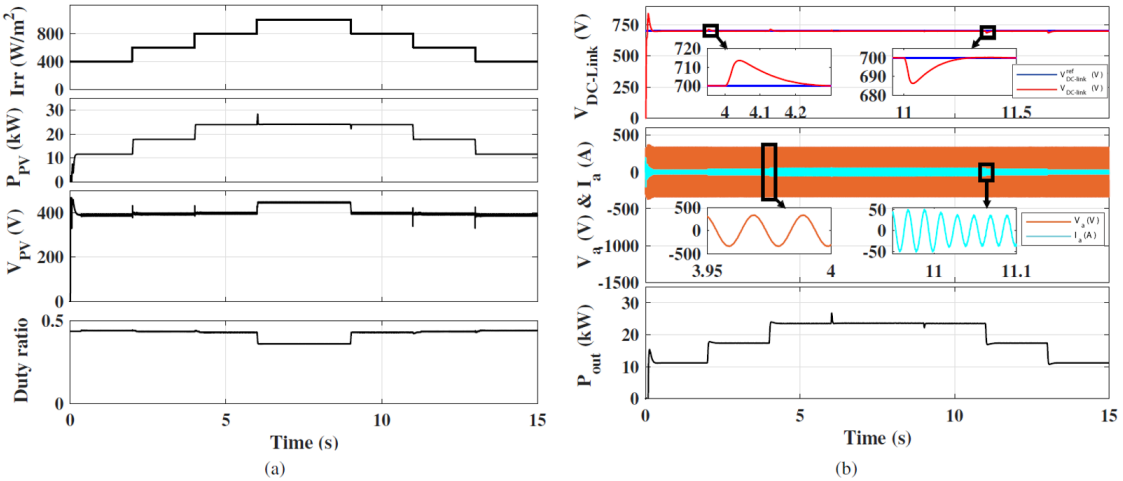

Fig. 12. Dynamic performance of modified P&O algorithm in derated power generation mode. (a) PV source output performances. (b) DC-link and inverter output performances.

TABLE I
PERFORMANCE ANALYSIS OF CONVENTIONAL AND MODIFIED P&O MPPT ALGORITHM

Sr. No.	Irradiance condition	Evaluation parameter	Mean and SD	Conventional P&O	Modified P&O
1	At constant irradiance condition (600 W/m^2)	$t_{s,V_{MPP}}$	Mean	0.768	0.61
			SD	2.2781×10^{-16}	1.1391×10^{-16}
		$t_{s,V^{ref}_{DC-link}}$	Mean	0.6312	0.57
			SD	0.000410391	1.13906×10^{-16}
2	At variable irradiance condition (600 to 400 W/m^2)	$t_{s,V_{MPP}}$	Mean	1.9365	1.768
			SD	0.03437793	0.00615587
		$t_{s,V^{ref}_{DC-link}}$	Mean	2.066	2.049
			SD	0	0.003077935
3	At variable irradiance condition (400 to 600 W/m^2)	$t_{s,V_{MPP}}$	Mean	3.265	3.237
			SD	4.55626×10^{-16}	0.03785012
		$t_{s,V^{ref}_{DC-link}}$	Mean	3.5319	3.39
			SD	0.004278465	4.55626×10^{-16}

V. CONCLUSION

A two-stage, three-phase, grid integrated PV system works in derated power generation mode to curtail the extra feed-in power during the peak hours. In addition, it avoids the drift phenomena which exists in traditional P&O algorithm. Furthermore, the proposed algorithm works in a modified MPPT mode during the non-peak hour. In this mode, the MPPT holds the information of current to distinguish irradiance change. Thus, it can estimate the direction of search towards MPP during irradiance change. Thereby, the operating point does not diverge from the shortest path of MPPT. Moreover, to enhance the tracking capability of the modified MPPT, it is examined on different step size (ΔD). In this paper, a large step size has been chosen which increases the time response and reduces the oscillation using the proposed algorithm. The system is implemented for 30 kW, two-stage, three-phase, GIPVS and simulated in MATLAB/Simulink environment using Simpower tools. The system's performanc-

es present that the proposed algorithm actively participates in power curtailment during the peak hours of power generation. Additionally, the performances show that the modified algorithm gives a faster response than the traditional P&O algorithm under variable irradiance condition.

REFERENCES

[1] O. Abedinia, D. Raisz, and N. Amjady, "Effective prediction model for hungarian small-scale solar power output," *IET Renewable Power Generation*, vol. 11, no. 13, pp. 1648-1658, 2017.

[2] O. Abedinia, N. Amjady, and N. Ghadimi, "Solar energy forecasting based on hybrid neural network and improved metaheuristic algorithm," *Computational Intelligence*, vol. 34, no. 1, pp. 241-260, 2018.

[3] F. Blaabjerg, Z. Chen, and S. B. Kjaer, "Power electronics as efficient interface in dispersed power generation systems," *IEEE Transactions on Power Electronics*, vol. 19, pp. 1184-1194, Sept. 2004.

[4] Q. Zhou and J. W. Bialek, "Generation curtailment to manage voltage constraints in distribution networks," *IET Generation, Transmission Distribution*, vol. 1, pp. 492-498, May 2007.

[5] R. Tonkoski, L. A. C. Lopes, and T. H. M. El-Fouly, "Coordinated active power curtailment of grid connected pv inverters for overvoltage prevention," *IEEE Transactions on Sustainable Energy*, vol. 2, pp. 139-147, Apr. 2011.

[6] W. A. Omran, M. Kazerani, and M. M. A. Salama, "Investigation of methods for reduction of power fluctuations generated from large grid-connected photovoltaic systems," *IEEE Transactions on Energy Conversion*, vol. 26, pp. 318-327, Mar. 2011.

[7] A. Ahmed, L. Ran, S. Moon, and J. Park, "A fast pv power tracking control algorithm with reduced power mode," *IEEE Transactions on Energy Conversion*, vol. 28, pp. 565-575, Sept. 2013.

[8] Y. Yang, H. Wang, F. Blaabjerg, and T. Kerekes, "A hybrid power control concept for pv inverters with reduced thermal loading," *IEEE Transactions on Power Electronics*, vol. 29, pp. 6271-6275, Dec. 2014.

[9] A. Sangwongwanich, Y. Yang, and F. Blaabjerg, "High-performance constant power generation in grid-connected pv systems," *IEEE Transactions on Power Electronics*, vol. 31, pp. 1822-1825, Mar. 2016.

[10] A. Sangwongwanich, Y. Yang, F. Blaabjerg, and H. Wang, "Benchmarking of constant power generation strategies for single-phase grid-connected photovoltaic systems," *IEEE Transactions on Industry Applications*, vol. 54, pp. 447-457, Jan. 2018.

[11] H. D. Tafti, A. I. Maswood, G. Konstantinou, J. Pou, and F. Blaabjerg, "A general constant power generation algorithm for photovoltaic systems," *IEEE Transactions on Power Electronics*, vol. 33, pp. 4088-4101, May 2018.

[12] S. Jain and V. Agarwal, "Comparison of the performance of maximum power point tracking schemes applied to single-stage grid-connected photovoltaic systems," *IET Electric Power Applications*, vol. 1, pp. 753-762, Sept. 2007.

[13] Z. Salam and J. Ahmed, "A modified p&o maximum power point tracking method with reduced steady-state oscillation and improved tracking efficiency," *IEEE Transactions on Sustainable Energy*, vol. 7, pp. 1506-1515, Oct. 2016.

[14] L. Zhang, S. S. Yu, T. Fernando, H. H.-C. Iu, and K. P. Womg, "An online maximum power point capturing technique for high-efficiency power generation of solar photovoltaic systems," *Journal of Modern Power Systems and Clean Energy*, vol. 7, pp. 357-368, Mar. 2019.

[15] T. Esram and P. L. Chapman, "Comparison of photovoltaic array maximum power point tracking techniques," *IEEE Transactions on Energy Conversion*, vol. 22, pp. 439-449, Jun. 2007.

[16] B. Subudhi and R. Pradhan, "A comparative study on maximum power point tracking techniques for photovoltaic power systems," *IEEE Transactions on Sustainable Energy*, vol. 4, pp. 89-98, Jan. 2013.

[17] M. Killi and S. Samanta, "Modified perturb and observe mppt algorithm for drift avoidance in photovoltaic systems," *IEEE Transactions on Industrial Electronics*, vol. 62, pp. 5549-5559, Sept. 2015.

[18] Y. Yang and H. Wen, "Adaptive perturb and observe maximum power point tracking with current predictive and decoupled power control for grid-connected photovoltaic inverters," *Journal of Modern Power Systems and Clean Energy*, vol. 7, pp. 422-432, Mar. 2019.

[19] F. Liu, S. Duan, F. Liu, B. Liu, and Y. Kang, "A variable step size inc mppt method for pv systems," *IEEE Transactions on Industrial Electronics*, vol. 55, pp. 2622-2628, Jul. 2008.

[20] A. Ghamrawi, J.-P. Gaubert, and D. Mehdi, "A new dual-mode maximum power point tracking algorithm based on the perturb and observe algorithm used on solar energy system," *Solar Energy*, vol. 174, pp. 508-514, 2018.

[21] F. Olivier, P. Aristidou, D. Ernst, and T. V. Cutsem, "Active management of low-voltage networks for mitigating overvoltages due to photovoltaic units," *IEEE Transactions on Smart Grid*, vol. 7, pp. 926-936, Mar. 2016.

[22] M. Shayestegan, "Overview of grid-connected two-stage transformerless inverter design," *Journal of Modern Power Systems and Clean Energy*, vol. 6, pp. 642-655, Jul. 2018.

[23] A. I. Ali, M. A. Sayed, and E. E. Mohamed, "Modified efficient perturb and observe maximum power point tracking technique for grid-tied pv system," *International Journal of Electrical Power & Energy Systems*, vol. 99, pp. 192-202, 2018.

[24] A. Ramyar, H. Iman-Eini, and S. Farhangi, "Global maximum power point tracking method for photovoltaic arrays under partial shading conditions," *IEEE Transactions on Industrial Electronics*, vol. 64, pp. 2855-2864, Apr. 2017.

[25] S. Liu, P. X. Liu, and X. Wang, "Stochastic small-signal stability analysis of grid-connected photovoltaic systems," *IEEE Transactions on Industrial Electronics*, vol. 63, pp. 1027-1038, Feb. 2016.

[26] V. Kumar and M. Singh, "Sensorless dc-link control approach for three-phase grid integrated pv system," *International Journal of Electrical Power & Energy Systems*, vol. 112, pp. 309-318, 2019.

[27] *o*X. Wang, F. Zhuo, J. Li, L. Wang, and S. Ni, "Modeling and control of dual-stage high-power multifunctional pv system in d - q - coordinate," *IEEE Transactions on Industrial Electronics*, vol. 60, pp. 1556-1570, Apr. 2013.

[28] A. K. Singh, I. Hussain, and B. Singh, "Double-stage three-phase grid-integrated solar pv system with fast zero attracting normalized least mean fourth based adaptive control," *IEEE Transactions on Industrial Electronics*, vol. 65, pp. 3921-3931, May 2018.

Vinit Kumar received the B.Tech. degree in electrical and electronics engineering from Rajasthan Technical University, Kota, India, in 2012, and the M.E. degree in power system, from the Thapar Institute of Engineering and Technology, Patiala, India, in 2015, where he is currently working toward the Ph.D. degree at the Department of Electrical and Instrumentation Engineering. His research interests include grid interfaced converters, photovoltaic systems and grid integration of renewable energy sources.

Mukesh Singh received the B.Tech. degree in electrical engineering from BIT, Sindhri, India, in 2000, the M.E. degree in electrical engineering from the Walchand College of Engineering, Sangli, India, in 2008, and Ph.D. degree from Indian Institute of Technology, Guwahati, India, in 2013. He is currently working as Associate Professor with the Department of Electrical and Instrumentation Engineering, Thapar Institute of Engineering and Technology, Patiala, India. His research interests include smart grid, electric vehicle, renewable energy sources and distributed generation.